Supporting Information

NIR-Triggered Photothermal Nanocomposite Hydrogels Integrating Polydopamine Carbon Dots and Dynamic Multi-Networks for Infected Wound Healing

Huanxuan Huang[a#], Shiyang Liao[b#], Dong Zhang[a], Hanwen Jiang[a], Qijia Liu[c,d], Keqing Xu[c*], Yunlong Sun[e*], Meidong Lang[a*]

[a] Shanghai Key Laboratory of Advanced Polymeric Materials, School of Materials Science and Engineering, East China University of Science and Technology, 130 Meilong Road, Shanghai 200237, China.

[b] Hebei Medical University, 361 East Zhongshan Road, Shijiazhuang 050017, China.

[c] Department of Orthopedics, The First Affiliated Hospital of Anhui University of Science and Technology, 203 Huaibin Road, Huainan 232000, China.

[d] Bengbu Medical University, 2600 Donghai Avenue, Bengbu 233030, China.

[e] R&D Center of Jiangxi Copper Co., Ltd., Nanchang 330096, China.

[*] Corresponding authors, E-mail address: mdlang@ecust.edu.cn

1. Characterization

1.1. Photothermal conversion efficiency

To quantitatively evaluate the photothermal conversion efficiency (η) of the PDA-CDs, the temperature profile during the laser heating and subsequent natural cooling phases was recorded. The η value was calculated according to the following established equations:

$$\tau_s = \frac{MC}{hs}$$

$$Q = hS(T_{max,water} - T_{surr})$$

$$\eta = \frac{hS(T_{max,PDA-CDs} - T_{surr}) - Q}{I(1 - 10^{-A808})}$$

where τ_s is the thermal time constant derived from the linear fit of the cooling curve. M and C denote the mass and specific heat capacity of the solvent (water), respectively. The term hS represents the heat transfer coefficient (h) multiplied by the surface area of the sample cell (S). T_{max} is the maximum temperature achieved under NIR irradiation, T_{surr} is the ambient surrounding temperature. Q represents the heat loss from the light absorption of the sample container, I is the incident laser power density, and A_{808} represents the absorbance of the PDA-CDs solution at 808 nm.

1.2. Rotational rheometer

The rheological behavior of the hydrogels at 37 °C was evaluated using a rotational rheometer (HAAKE MARS III) in oscillatory frequency sweep mode. The frequency range was set from 0.1 to 10 Hz with a constant strain of 1%.

1.3. Swelling Capacity

For swelling kinetics assessment, hydrogel samples were immersed in PBS (pH 7.4) and the weights of the swollen samples were recorded at predetermined time points. The swelling ratio was calculated using the following equation:

$$Swelling\ Ratio\ (\%) = \frac{W_s - W_0}{W_0} \times 100\%$$

where W_0 and W_s represent the weights of the hydrogels before and after swelling, respectively.

1.4. Release kinetics of hydrogels encapsulated PDA-CDs

PDA-CDs release behavior was quantified using a standard calibration curve established at 350 nm via UV-vis spectroscopy. Briefly, a PDA-CDs solution and the OG/PCDs hydrogel (equally loaded with PDA-CDs) were enclosed in dialysis bags (MWCO = 3500 Da) and incubated in 50 mL of PBS in a shaking incubator at 37 °C. To evaluate the pH-responsive release profile, the experiments were conducted at pH 7.4 and 5.4, simulating the physiological conditions and the acidic microenvironment typical of infected wounds, respectively. At predetermined intervals, 5 mL of the release medium was collected and replenished with fresh PBS. The concentration of PDA-CDs was measured using a microplate reader, and the cumulative release was determined based on the standard curve and the following equations:

$$Cumulative\ release\ (\%) = \frac{5 \times \sum_{n+1}^{n-1} C_i + 50 \times C_i}{m} \times 100\%$$

Where C_i denotes the concentration of PDA-CDs in the medium collected at the i-th sampling step, and m represents the total mass of PDA-CDs.

1.5. Cell cytotoxicity assay

The cytocompatibility of the hydrogels was evaluated using L929 fibroblasts. Hydrogel extraction media were prepared by incubating the hydrogels in DMEM at 37 °C for 24 h, adhering to the ISO 10993-12:2021 standard. Cells were seeded in 96-well plates at a density of 2 $\times 10^3$ cells per well and cultured for 24 h. Subsequently, the original culture medium was replenished with the harvested hydrogel extracts for further incubation. After 1, 3, and 5 days of incubation, cell viability were quantitatively assessed via the Cell Counting Kit-8 (CCK-8) assay by measuring the absorbance at 450 nm. Each sample was prepared in quintuplicate (n = 4). To visually assess cell viability, Calcein-AM/PI Live/Dead kits were performed on day 3, and the stained cells were imaged using CLSM.

1.6. Hemolysis assay

To determine the hemocompatibility of the hydrogels, hydrogels were then co-incubated with prepared RBC suspension (4% in saline) at 37 °C for 1 h. Saline and deionized water were employed as the negative and positive controls, respectively.

After incubation, the mixtures were centrifuged, and the absorbance of the supernatant was measured at 540 nm. Each sample was prepared in quintuplicate (n = 4). The hemolysis rate was calculated according to the following equation:

$$Hemolysis\ (\%) = \frac{OD_{Sample} - OD_{Negative}}{OD_{Positive} - OD_{Negative}} \times 100\%$$

where OD_{Sample}, $OD_{Negative}$, and $OD_{Positive}$ represent the absorbance values of the experimental group, negative control, and positive control, respectively.

2. Results and discussion

Table. S1. Minimum inhibitory concentrations and selectivity index values.

Sample	MIC (μg/mL)	
	S. aureus	***E. coli***
PDA	2000	2000
PDA-CDs	250	250
PDA-CDs+NIR	125	250

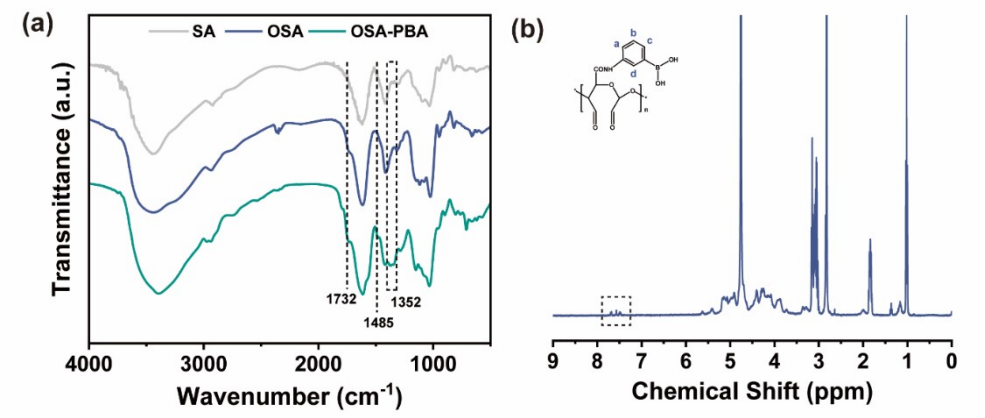

Fig. S1. (a) FT-IR spectra of SA, OSA and OSA-PBA. (b) ^{1}H NMR spectra of OSA-PBA.

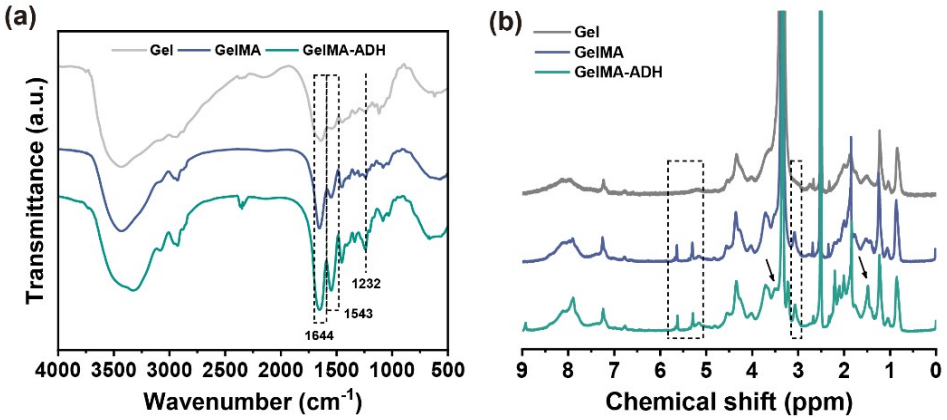

Fig. S2. (a) FTIR spectra and (b) ^{1}H NMR spectra of the Gel, GelMA and GelMA-ADH.

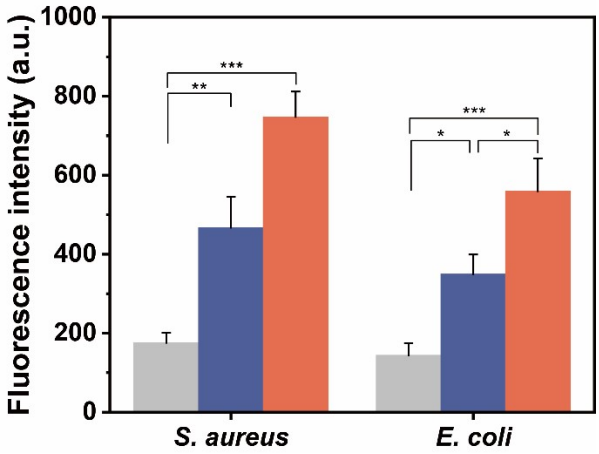

Fig. S3. The fluorescence intensity of bacterial cell membrane potential levels using DiSC3(5) as probe. The data are presented as mean ± S.D. ($n = 3$). *$p < 0.05$; ** $p < 0.01$, *** $p < 0.001$.

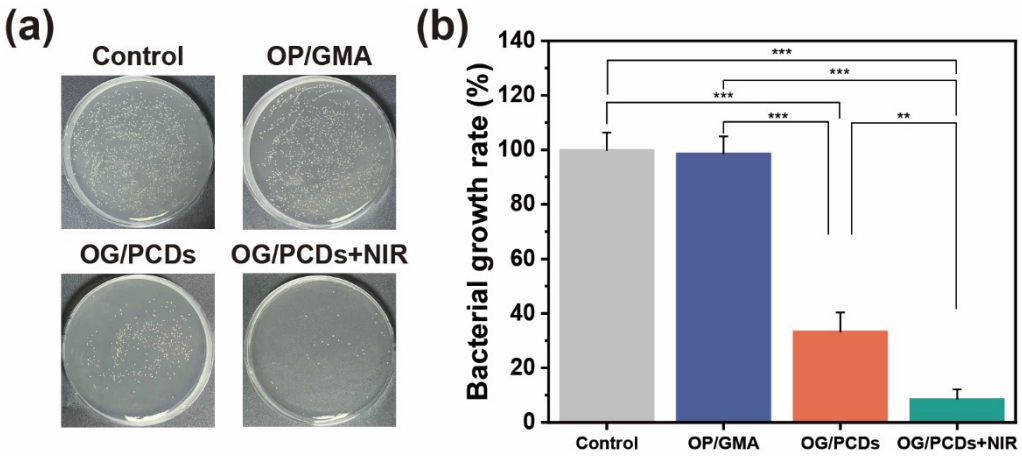

Fig. S4. (a) Representative photographs of CFU agar plates and (b) bacterial viability of mature biofilm after co-culture with hydrogels. The data are presented as mean ± S.D. ($n = 3$). ** $p < 0.01$, *** $p < 0.001$.

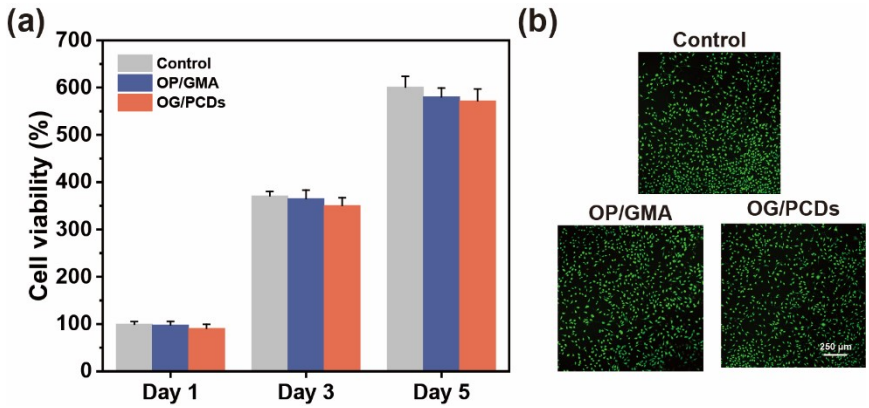

Fig. S5. (a) Cell viability in different groups. (b) Live/Dead staining fluorescence images after treated for 3 days. Scale bar: 250 μm. The data are presented as mean ± S.D. ($n = 4$).

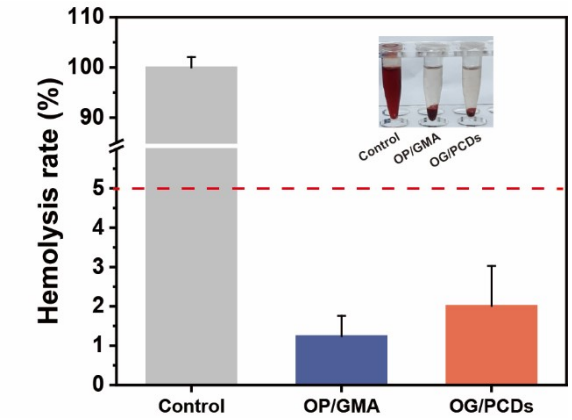

Fig. S6. Hemolysis rate of the hydrogels. The data are presented as mean ± S.D. ($n = 4$).

.

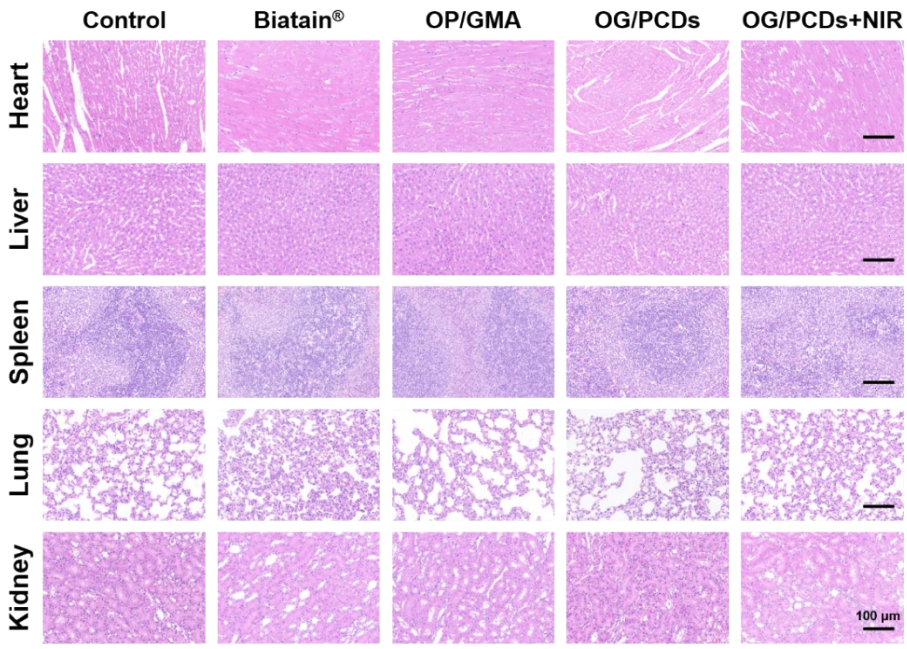

Fig. S7. Representative H&E staining images of major organs in different treatment groups. Scale bar: 100 μm.

Table. S2. Comparison of photothermal antibacterial hydrogel dressings for infected wounds management.

Hydrogel System	**PTAs**	**Photothermal conversion Efficiency**	**Infected Model**	***In Vivo* Antibacterial Rate**	**Wound Closure Rate**	**Ref.**
OG/PCDs (This work)	PDA-CDs	56.90%	*S. aureus*	99.68%	98.42%	
ML-OCP	MPDA	—	*S. aureus*	99.45%	96.60%	[1]
QP/QT-MB	MPDA	—	*S. aureus*	97.60%	97.70%	[2]
MS@Chl@Ag	Ag NPs	25.44%	*S. aureus*	—	97.74%	[3]
CAP@MXene/CuTCPP	MXene	44.51%	*MRSA*	—	98.81%	[4]
STB-Lid	TPT-B_{12}	—	*S. aureus*	97.90%	97.00%	[5]
GPC-BTC	BPNS	29.30%	*S. aureus* (burn)	—	~90.00%	[6]

References

1. Zhu, H.; Wang, L.; Xu, K.; Wang, X.; Hu, B.; Li, W.; Cao, J.; Yuan, Y., A Multifunctional Nanocomposite Hydrogel Platform with a Sequentially Coordinated Strategy for Infected Wound Healing. *ACS Applied Materials & Interfaces* **2026,** *18* (14), 20146-20158.

2. Peng, W.; Li, L.; Zhang, Y.; Su, H.; Jiang, X.; Liu, H.; Huang, X.; Zhou, L.; Shen, X.-C.; Liu, C.; Peng, W., Photothermal synergistic nitric oxide controlled release injectable self-healing adhesive hydrogel for biofilm eradication and wound healing. *Journal of Materials Chemistry B* **2024,** *12* (1), 158-175.

3. Li, J.; Ma, Y.; Le, Y.; Guo, Z.; Wang, Y.; Zheng, Y.; Xiao, S., Synergistic MS@Chl@Ag Composite System for Photothermal Antibacterial Therapy and Immune Microenvironment Modulation in Infected Wounds. *ACS Applied Materials & Interfaces* **2026,** *18* (1), 810-826.

4. Li, C.; Chang, Z.; Zhang, Y.; Shen, S.; Liu, L.; Zeng, D.; Fan, D., Bio-heterojunction-engineered recombinant collagen hydrogel orchestrates multimodal sterilization and immunomodulation for MRSA-infected wound healing. *Bioactive Materials* **2026,** *62*, 229-247.

5. Zhou, N.; Wang, W.; Xu, L.; Zhang, A.; Lu, X.; Chen, Y.-P.; Fan, S.; Zhang, T.; Yu, C.; Wang, X.-Q.; Fu, D., Analgesic-loaded NIR-II photothermal hydrogel for efficient anti-infection and precise pain management in wounds. *Materials Today Bio* **2026,** *37*, 102995.

6. Sang, Y.; Wang, J.; Wu, R.; Zhang, H.; Zheng, B.; Wang, B.; Hu, Y.; Li, L.; Liu, Z., Tannic acid-copper ion@black phosphorus doped cationic guar gum/polyvinyl alcohol nanocomposite hydrogel for burn wound healing with antioxidant and photothermal antibacterial activities. *International Journal of Biological Macromolecules* **2026,** *357*, 151647.